# CEACAM1 isoforms with different cytoplasmic domains show different localization, organization and adhesive properties in polarized epithelial cells

**Ulla Sundberg and Björn Öbrink***

Department of Cell and Molecular Biology, Medical Nobel Institute, Karolinska Institutet, Stockholm, Sweden
Author for correspondence (e-mail: bjorn.obrink@cmb.ki.se)

*Accepted 13 December 2001*
*Journal of Cell Science 115, 1273-1284 (2002) © The Company of Biologists Ltd*

## Summary

**CEACAM1 is a signaling cell adhesion molecule expressed in epithelia, vessel endothelia and leukocytes. It is expressed as two major isoforms with different cytoplasmic domains. CEACAM1 occurs both in cell-cell contact areas and on apical surfaces of polarized epithelial cells, but it is not known how the different isoforms are distributed in polarized cells or what the functions of CEACAM1 are in the apical surfaces. We investigated the localization and organization of the two CEACAM1 isoforms in transfected, polarized MDCK cells by confocal microscopy and differential surface labelling. CEACAM1-L was found on both the apical and the lateral surfaces, whereas CEACAM1-S appeared exclusively on the apical surfaces. Maintenance of the lateral localization of CEACAM1-L required homophilic binding between CEACAM1-L molecules on adjacent cells. Double-labelling with anti-CEACAM1 antibodies directed against different epitopes indicated that apical CEACAM1-L occurred either in a homophilic adhesive state or in a free non-adhesive state. CEACAM1-S appeared almost exclusively in the homophilic adhesive state. These findings suggest that CEACAM1 mediates adhesive bonds between adjacent microvilli on the apical surfaces.**

Key words: CEACAM1, Cell adhesion, Cell polarization, Microvilli, Signal transduction

## Introduction

CEACAM1 (carcinoembryonic antigen-related cell adhesion molecule 1), previously known as C-CAM, BGP and CD66a, is a member of a family of alternatively spliced cell adhesion molecules belonging to the immunoglobulin superfamily (Öbrink, 1997). It has been demonstrated that CEACAM1 can mediate intercellular adhesion of hepatocytes and several other cell types, including transfected cell lines, in vitro by homophilic binding between its N-terminal Ig-domains (Wikström et al., 1996). In adult organisms, CEACAM1 is abundantly expressed in liver, various epithelia, vessel endothelial cells, platelets and leukocytes (Odin et al., 1988). During embryonic development CEACAM1 appears early and becomes expressed also in other cell types, the most striking example being trophoblasts both of the preimplanting embryo and of the placenta (Sawa et al., 1997). CEACAM1 controls signal transduction and has important regulatory activities in cell proliferation (Singer et al., 2000), apoptosis (Huang et al., 1999), angiogenesis (Ergün et al., 2000), tumor growth (Hsieh et al., 1995; Kunath et al., 1995) and epithelial cell polarization (Huang et al., 1999). These regulatory activities seem to be associated with the ability of its cytoplasmic domains to bind to and interact with cytoplasmic protein tyrosine kinases (Brümmer et al., 1995; Skubitz et al., 1995) and protein tyrosine phosphatases (Huber et al., 1999), as well as with calmodulin (Edlund et al., 1996) and actin (Sadekova et al., 2000).

The subcellular location of CEACAM1 exhibits interesting differences between cell types (Odin et al., 1988; Sawa et al., 1994). In stratified epithelia, CEACAM1 is present on the cell surface in cell contact areas. In brush-border-carrying simple epithelia, it is most abundant in the apical surfaces. In the mature liver, it is highly expressed in bile canalicular membranes. In the vascularizing central nervous system, it appears in contact areas between endothelial cells and pericytes. And in non-activated polymorphonuclear neutrophils and platelets, it is present in intracellular membranes that fuse with the plasma membrane upon activation.

The expression of CEACAM1 in the apical surfaces of the simple epithelia of the small intestine and the proximal kidney tubules and in the bile canaliculi of mature hepatocytes has cast doubts on the adhesive function of CEACAM1 in these cells, because this location was not expected for a molecule that is involved in cell-cell adhesion. However, bile canaliculi go through contraction-relaxation cycles (Phillips et al., 1982; Watanabe et al., 1991), and in the contracted phase, the bile canalicular membranes are organized in microvillar structures, the membranes of which are in close contact with each other (Watanabe et al., 1991). Also the microvillar membranes of the brush borders of the apical surfaces of the intestinal and tubular epithelial cells show close contacts (Copenhaver et al., 1971). Therefore, an adhesive function of CEACAM1 cannot be ruled out in these locations. Another issue that has not yet been satisfactorily solved is whether CEACAM1 is also present in the lateral membranes of simple epithelial cells. By immunohistochemistry, a weak staining for CEACAM1 was observed in rat intestinal epithelial cells (Hansson et al., 1989) and in human mammary epithelial cells (Huang et al., 1999). Furthermore, Mowery and Hixson (Mowery and Hixson,

1991), applying fixation and mechanical dissociation of mature rat liver, demonstrated that CEACAM1 was also present in the lateral membranes between adjacent hepatocytes, in addition to its expression in the canalicular membranes. Thus, it seems that CEACAM1 can occur at the lateral surfaces of polarized epithelial cells but that some of its epitopes may be masked.

The two major isoforms of CEACAM1 are CEACAM1-L and CEACAM1-S, which differ in their cytoplasmic domains owing to differential splicing of one exon (Edlund et al., 1993). Both cytoplasmic domains can be phosphorylated on serine residues (Odin et al., 1986; Edlund et al., 1998) and can bind to calmodulin in a calcium-regulated manner (Edlund et al., 1996). The cytoplasmic L domain, which consists of 71 amino acids, has two tyrosine residues, which upon phosphorylation can recruit and activate src-family kinases (Brümmer et al., 1995) or the protein tyrosine phosphatases SHP-1 and SHP-2 (Huber et al., 1999). The 10 amino-acid long cytoplasmic S domain lacks these tyrosine residues. CEACAM1-L and CEACAM1-S are co-expressed in CEACAM1-expressing cells, but the expression ratios vary between different cell types and between different cellular states (Baum et al., 1996; Singer et al., 2000). Since six of the amino acids in the 10 amino-acid long S domain are identical to the sequence of the L domain, it has been difficult to produce antibodies that efficiently can distinguish between the two isoforms in situ. Therefore, it is not known whether they are distributed in an identical fashion in the apical and lateral surfaces of polarized epithelial cells. This is, however, an important issue since CEACAM1 participates in signal regulation, and CEACAM1-S can regulate the signaling activities of CEACAM1-L (Öbrink, 1997). Thus, it is crucial to know the relative expression of each isoform in different parts of polarized epithelial cells.

In the present work we have addressed four questions: 1) What is the surface location of CEACAM1 in highly polarized epithelial cells that have distinct apical and basolateral surfaces? 2) Is there any difference in the surface location of the two isoforms CEACAM1-L and CEACAM1-S? 3) Do the two CEACAM1 isoforms interact differently with the plasma membrane cortex? 4) Is CEACAM1 involved in adhesive interactions in highly polarized epithelial cells? We demonstrate that the two isoforms localized differently in polarized MDCK cells. CEACAM1-L occurred both on the lateral and the apical surfaces, whereas CEACAM1-S became expressed exclusively on the apical surfaces. The N-domain of the laterally expressed CEACAM1-L was masked, indicating that this isoform at this location participates in homophilic cell-cell adhesion. Furthermore, apically expressed CEACAM1 exhibited both masked and unmasked states of the N-domain, indicating that CEACAM-1 participates in adhesive interactions also in this location.

## Materials and Methods

### Antibodies

Affinity-purified, rabbit polyclonal antibodies (αCC16) against rat CEACAM1 and Fab fragments were produced and characterized as previously described (Ocklind and Öbrink, 1982; Odin et al., 1986). The mouse Mab 5.4, recognizing the N-terminal immunoglobulin domain of rat CEACAM1 (Singer et al., 2000), was generously provided by D.C. Hixson, Rhode Island Hospital, Brown University, Providence, RI. The mouse monoclonal antibody against occludin was from Zymed Laboratories, Inc. FITC-conjugated swine anti-rabbit antibodies and horseradish peroxidase-labeled swine anti-rabbit antibodies were from Dako. Alexa488-conjugated goat anti-mouse IgG $F(ab')_2$ and Alexa546-conjugated goat anti-rabbit IgG were from Molecular Probes.

### Cell culture and transfection

MDCK II cells were grown in a 5% $CO_2$ humidified athmosphere at 37°C in DMEM supplemented with 10% heat-inactivated fetal bovine serum, 100 U/ml penicillin and 100 mg/ml streptomycin. They were transfected by the calcium phosphate precipitation method (10 μg of cDNA for CEACAM1-L or CEACAM1-S in the pRAX vector plus 1 μg of a cDNA coding for the neomycin resistance gene), selected in 0.5 mg/ml G418 for 14 days and cloned by limiting dilution as previously described (Olsson et al., 1995). Cell polarization was achieved by growth for 3 days on permeable filter inserts (Falcon, PET filters 0.45 μm pore size, cat. no. 3090) that separated the apical and basolateral compartments. Formation of tight monolayers was monitored by $^3$H-inulin that was added to the upper compartment (Caplan et al., 1986). Only cell layers that permitted passage of less than 1% of the inulin from the upper to the lower compartment were used for experiments.

### Cell solubilization

Cells on tissue culture dishes were solubilized at room temperature with varying concentrations of Triton X-100 in Buffer P (150 mM NaCl, 25 mM Hepes pH 7.4, 5 mM EGTA, 10 mM $Na_4P_2O_7$, 50 mM NaF, 1 mM $Na_3VO_4$, 0.5 mM AEBSF, 1000 KIE/ml aprotinin and 1μg/ml leupeptin, 1 μg/ml pepstatin). Supernatants from the solubilized cells were immunoprecipitated with αCC16 at 4°C overnight and protein A-Sepharose. The immunoprecipitates and the detergent-insoluble cell residues were solubilized in a 1:1 mixture of Buffer P/2% SDS and 2× SDS sample buffer, reduced with 50 mM DTT at room temperature for 4 hours, heated at 100°C for 5 minutes and subjected to SDS-PAGE on 7% polyacrylamide gels (Laemmli, 1970).

### Biochemical surface localization

Tight monolayers of MDCK cells polarized on permeable insert filters were incubated for 2 hours at 4°C with αCC16 Fab fragments added from either the upper, apical compartment or the lower, basolateral compartment. The cell layers were washed three times with PBS/1mM $CaCl_2$/1mM $MgCl_2$ and were then solubilized in 1% Triton X-100 in Buffer A (150 mM NaCl, 20 mM Tris-HCl pH 8.0, 5 mM EDTA, 0.2% BSA, 1 mM PMSF, 1000 KIE/ml aprotinin) for 1 hour at 4°C and centrifuged at 14000 ***g*** for 15 minutes. The supernatants were incubated with swine anti-rabbit IgG (DAKO A/S, Denmark) overnight at 4°C, followed by incubation with protein A Sepharose for 30 minutes. The beads were collected by centrifugation, washed once with Buffer A, three times with 1% Triton X-100/0.1% SDS in Buffer A, three times with 0.5% Triton X-100 in Buffer C (500 mM NaCl, 20 mM Tris-HCl, pH 8.0, 0.2% BSA) and once in 50 mM Tris-HCl, pH8.0. The immunoprecipitates were recovered from the washed beads by solubilization in 1× SDS sample buffer, reduced with 50 mM DTT, heated at 100°C for 5 minutes and analyzed by SDS-PAGE on 7% polyacrylamide gels and immunoblotting with αCC16.

### Immunoblotting

Proteins separated by SDS-PAGE were transferred to nitrocellulose membranes, blocked in 5% defatted milk powder in TBS/0.05% Tween 20, pH 7.4 and incubated with αCC16 for 1 hour at room temperature, followed by horseradish-peroxidase-labeled swine anti-rabbit antibodies and developed by ECL. The developed films were scanned in a gel documentation equipment (Herolab) and processed in Photoshop 6 (Adobe).

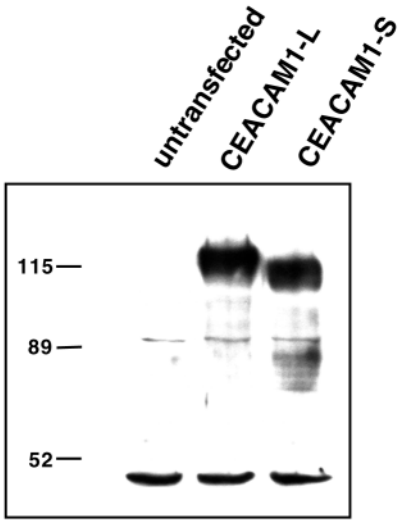


**Fig. 1.** Expression of CEACAM1 in transfected MDCK cells. Untransfected MDCK cells and MDCK cells transfected with CEACAM1-L or CEACAM1-S were analyzed by immunoblotting using αCC16 antibodies for development. The CEACAM1-L-transfected cells expressed a 120 kDa immunoreactive protein and the CEACAM1-S-transfected cells expressed a 115 kDa immunoreactive protein, whereas untransfected MDCK cells had no immunoreactive protein in the 100-120 kDa range. The molecular masses (in kDa) of marker proteins are shown to the left.

### Confocal microscopy

Tight monolayers of MDCK cells polarized on permeable insert filters were fixed with 3% paraformaldehyde for 30 minutes at room temperature. The cell layers were permeabilized with Triton X-100 or methanol (described in detail in Results), and reactive aldehyde groups were quenched in 50 mM $NH_4Cl$ for 15 minutes at room temperature. In some experiments, the cells were treated with hyperosmotic sucrose (1 M sucrose in PBS for 30 minutes at 37°C) before fixation and permeabilization. The cells were then incubated overnight at 4°C with primary antibodies (affinity purified αCC16, Mab 5.4, anti-occludin antibody) followed by secondary antibodies for 1 hour at room temperature and were examined with a Zeiss LSM 510 scanning module fitted to an Axiovert 100 M microscope using a 63× oil immersion objective. Routinely, 0.35 μm thick focal planes were scanned. The data files were processed with the LSM software and transferred to PowerPoint (Microsoft).

## Results

### CEACAM1 expression

Rat CEACAM1 was transfected into MDCK cells. Untransfected MDCK cells did not react with antibodies against rat CEACAM1 either in immunoblotting (Fig. 1; the bands of approximately 90 kDa and 50 kDa showed up also when pre-immune immunoglobulins were used) or in immunofluorescence (Fig. 7). After transfection and selection, several clones were obtained that were positive for CEACAM1-L and CEACAM1-S, respectively. Three independent clones of CEACAM1-L- (F6H12; 1.0H4; 1.0H8) and CEACAM1-S- (E10H8; 0.7H4; 1.0G10) transfected cells, respectively, were selected for further analyses. All clones exhibited identical cell surface distribution of respective CEACAM1 isoform; experimental data are only shown for clones F6H12 and E10H8. Immunoblotting revealed expression of a 120 kDa protein in the CEACAM1-L transfected cells and a protein of slightly smaller size, as expected, in the CEACAM1-S transfected cells (Fig. 1). Immunofluorescence analysis of non-permeabilized cells showed that both proteins were expressed on the cell surface (Figs 3, 5).

### Solubility of surface-localized CEACAM1

Immunofluorescence of transfected cells grown on regular Petri dishes revealed a striking difference in the extractability of CEACAM1-L and CEACAM1-S (data not shown). Thus, treatment of cells that had been fixed with 2% paraformaldehyde for 30 minutes and with 0.1% Triton X-100 for 30 minutes resulted in a complete loss of immunoreactive staining for CEACAM1-S, whereas the staining for CEACAM1-L remained to a large extent, particularly at the lateral cell surfaces. This result indicated that a portion of CEACAM1-L was associated with the cell cortex, that is the plasma membrane and the underlying actin filament network, in a different way from CEACAM1-S.

The finding that detergent treatment caused loss of CEACAM1 even after fixation, and that this affected the two isoforms differently, prompted a detailed investigation of the fixation and permeabilization conditions in order to find a procedure in which no CEACAM1 of either isoform was lost, while at the same time maximal antibody binding for efficient staining was preserved. To that end we used combinations of paraformaldehyde as fixative and Triton X-100 or methanol as permeabilizing agents and varied both the concentrations and time of treatment for both the fixative and the permeabilizing agents. The solubilization of the two CEACAM1 isoforms was analyzed by immunoblotting. When unfixed cells were treated with different concentrations of Triton X-100, we found that CEACAM1-L was more firmly bound in the cell cortex than CEACAM1-S. Thus, incubation at room temperature with 0.5% Triton X-100 for 10 minutes solubilized all of CEACAM1-S, whereas a significant portion of CEACAM1-L remained insoluble after incubation with 1% Triton X-100 (Fig. 2A). Both isoforms could be solubilized to some extent even after fixation with 3% paraformaldehyde, and CEACAM1-S was still more easily solubilized than CEACAM1-L (Fig. 2A). In order to completely prevent CEACAM1-S solubilization the cells had to be fixed with 4% paraformaldehyde for 60 minutes (data not shown). However, when methanol was used for permeabilization instead of Triton X-100, it was enough to fix the cells with 3% paraformaldehyde for 30 minutes to prevent CEACAM1 solubilization (Fig. 2A). The different fixation and permeabilization conditions were also applied to polarized cells, which demonstrated that the most efficient immunostaining was obtained by permeabilization with methanol for 2 minutes at room temperature (Fig. 2B).

### The surface location of CEACAM1-L and CEACAM1-S differs in polarized MDCK cells

The surface location of CEACAM1-L and CEACAM1-S was analyzed by confocal microscopy of fully polarized MDCK cells. Even if it was possible to immunostain cell surface molecules both on the apical and the basolateral surfaces by applying antibodies from either side, we found that the staining

was more efficient if the cells were permeabilized before addition of the antibodies, since we used filters with low pore density, which restricted the diffusion of the antibodies through the filters. In order to prevent loss of CEACAM1 by the permeabilization procedure, we routinely fixed the cells with 3% paraformaldehyde for 30 minutes and permeabilized them by treatment with methanol for 2 minutes at room temperature.

Antibody staining of confluent unpermeabilized cell monolayers utilizing polyclonal antibodies showed a strong expression of both CEACAM1-L and CEACAM1-S on the apical surfaces (Fig. 3). However, when the cell monolayers were permeabilized with methanol to allow efficient access of the antibodies to beneath the tight junctions, CEACAM1-L-expressing cells but not CEACAM1-S-expressing cells were strongly stained on their lateral surfaces (Fig. 2B, Fig. 3).

In order to obtain further proof of the different localization patterns of the two CEACAM1 isoforms seen by confocal microscopy, we designed a biochemical labelling technique. Viable, polarized and tight MDCK cell layers were incubated with αCC16 Fab fragments that were added either from the apical compartment or from the basolateral compartment. Fab fragments instead of intact immunoglobulins were used to facilitate rapid penetration through the filters and between the cells. After washing and solubilization of the cells, cell-bound Fab fragments were retrieved with anti-Fab antibodies and protein A-Sepharose, and Fab-complexed CEACAM1 was detected by immunoblotting. Using this procedure, CEACAM1-S was only retrieved from the apical surface, whereas CEACAM1-L could be retrieved both from the apical and the basolateral surfaces (Fig. 4). Thus, in agreement with the results of the confocal microscopy, this analysis also demonstrated that CEACAM1-L was expressed both on the lateral and the apical cell surfaces, whereas CEACAM1-S was localized exclusively to the apical surfaces. In addition, this experiment demonstrated that both isoforms were indeed exposed on the extracellular face of the plasma membrane.

The apical staining of both CEACAM1-L and CEACAM1-S appeared in a layer with a vertical height of 1-2 μm (Fig. 2B, Figs 3, 5-7). Polarized MDCK cells have a dense layer of uniform 1-2 μm long microvilli on their apical surfaces (Butor and Davoust, 1992). Thus, the confocal microscopical data

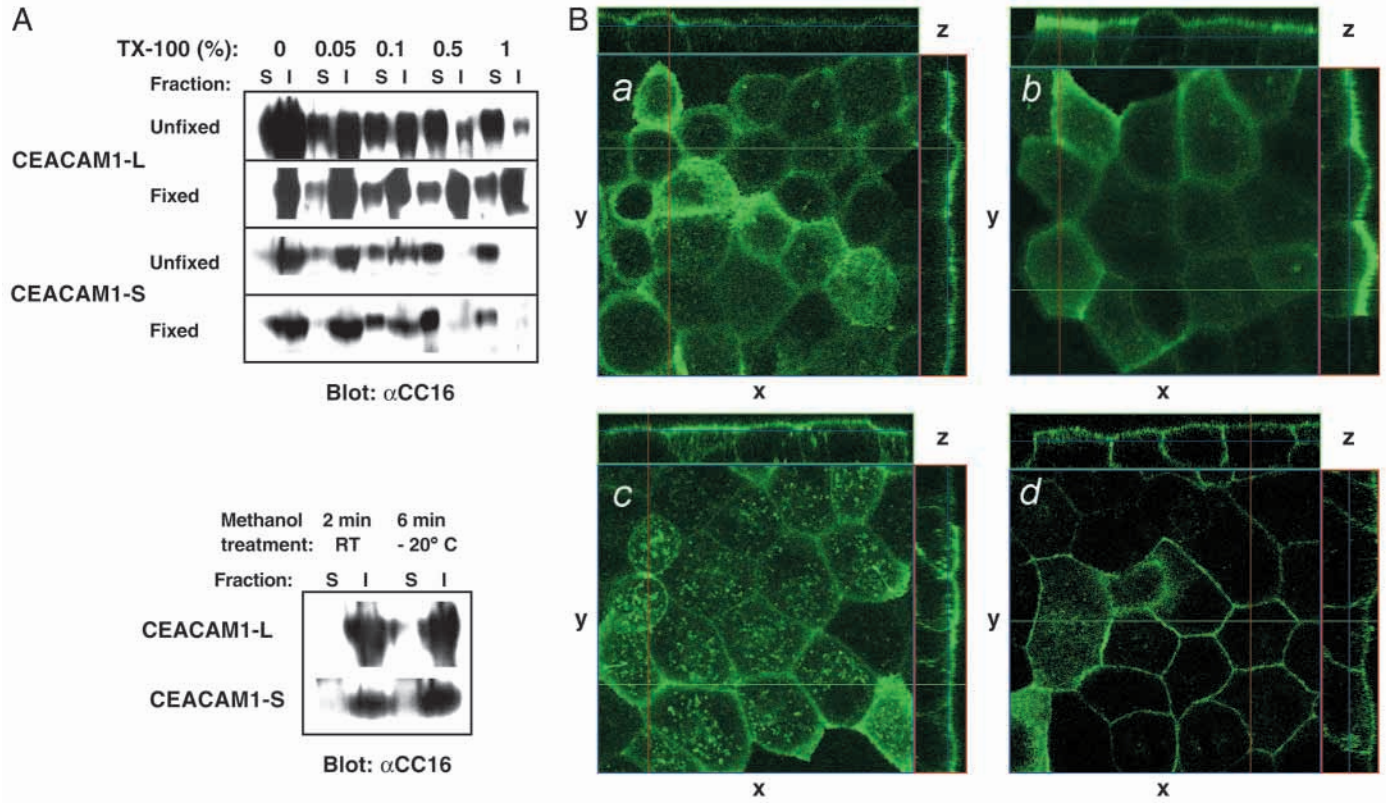


**Fig. 2.** Extractability of CEACAM1-L and CEACAM1-S. (A) Cells were grown on Petri dishes. Fixation was performed with 3% paraformaldehyde for 30 minutes. Upper panel: the cells were extracted with the indicated concentrations of Triton X-100 for 10 minutes at room temperature, and the soluble (S) and insoluble (I) fractions were analyzed by immunoblotting. Lower panel: fixed cells were extracted with absolute methanol for 2 minutes at room temperature or for 6 minutes at –20ºC, and the soluble (S) and insoluble (I) fractions were analyzed by immunoblotting. (B) CEACAM1-L-transfected cells were grown on permeable filters, fixed with 3% paraformaldehyde for 30 minutes, stained by αCC16 after the indicated permeabilization procedure and viewed by confocal microscopy. (a) Permeabilization with 0.05% Triton X-100 for 10 minutes. (b) Permeabilization with 0.1% Triton X-100 for 10 minutes. (c) Permeabilization with methanol for 6 minutes at –20ºC. (d) Permeabilization with methanol for 2 minutes at room temperature. Permeabilization with methanol for 2 minutes at room temperature gave the best preservation of the lateral staining of CEACAM1-L. The xy-fields represent the image in one focal plane (the xy-dimension) parallel to the basal surfaces (the filter plane) of the cells. The images labelled z represent the third, vertical z-dimension, obtained by computer reconstruction of all the focal planes analyzed in the xy-dimension. The lines in the xy-fields indicate the vertical planes that are shown in the z-reconstructions. The lines in the z-reconstructions indicate the level of the focal planes shown in the xy-fields.

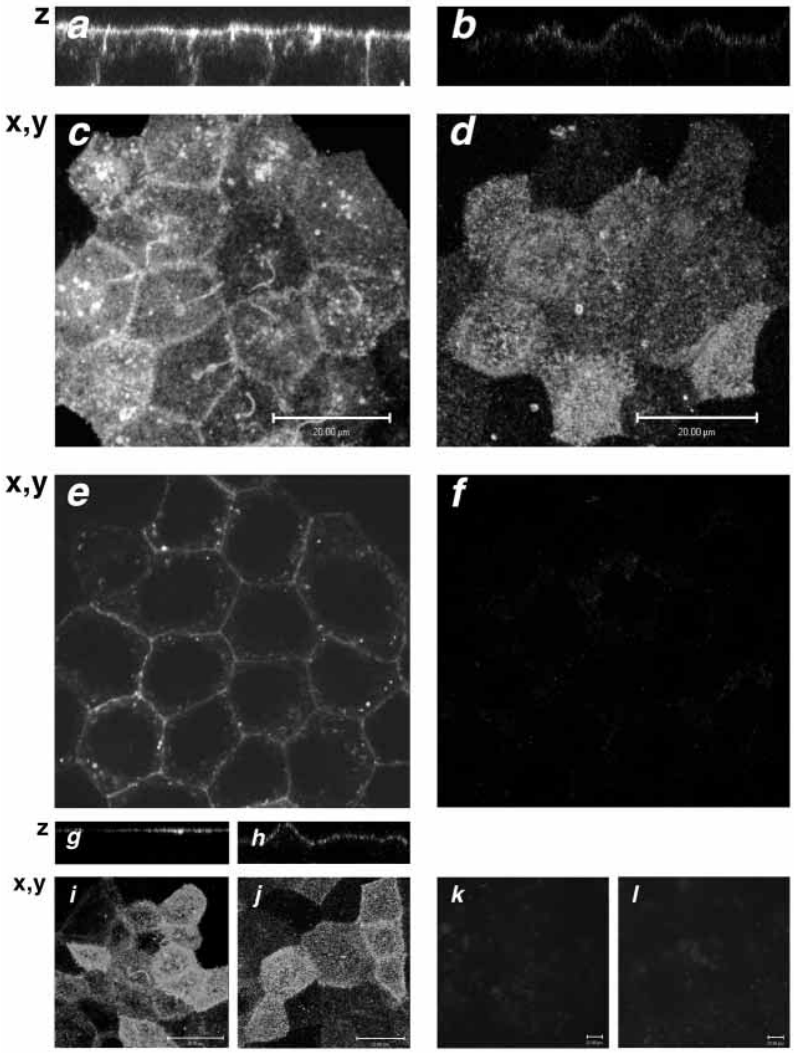


**Fig. 3.** Confocal microscopy of polarized CEACAM1-L and CEACAM1-S expressing MDCK cells. CEACAM1-L- (a,c,e,g,i,k) and CEACAM1-S- (b,d,f,h,j,l) expressing cells were immunostained with anti-CEACAM1 αCC16 antibodies (a-j) or pre-immune immunoglobulins (k,l) and FITC-labelled secondary antibodies. The cells were either permeabilized (a-f) by methanol for 2 minutes at room temperature or unpermeabilized (g-l) before staining. (a) is a z-reconstruction of the cells shown in xy-projections in (c) and (e), (b) is a z-reconstruction of the cells shown in xy-projections in (d) and (f), (g) is a z-reconstruction of the cells shown in xy-projection in (i), and (h) is a z-reconstruction of the cells shown in xy-projection in (j), respectively. The focal planes of (c,d,i,j,k,l) run through the apical cell surfaces. The focal planes of (e) and (f) run in the middle, between the apical and the basal cell surfaces. Apical staining for CEACAM1-L and CEACAM1-S is seen under all conditions, but lateral staining is only seen for CEACAM1-L and under permeabilizing conditions (a,e). Note that there is no lateral staining for CEACAM1-S (b and f). Bars: 20 µm.

demonstrated that both CEACAM1-L and CEACAM1-S were localized along the entire length of the apical microvilli.

### Lateral localization of CEACAM1-L requires cell-cell contact between CEACAM1-L-expressing cells

CEACAM1 can appear both as monomers and parallel dimers in the plane of the membrane (Hunter et al., 1996) and the N-terminal Ig-domain mediates homophilic adhesion by a reciprocal binding to an N-terminal Ig-domain presented by an adjacent membrane (Wikström et al., 1996). Therefore, it was of interest to use a monoclonal antibody specifically recognizing the N-terminal Ig-domain in the localization studies by confocal microscopy. Using Mab 5.4 we found a staining pattern that was strikingly different from that obtained with the polyclonal antibody αCC16. Although a significant portion of CEACAM1-L-expressing cells were stained on their apical surfaces, there was no lateral surface staining after methanol-permeabilization of the polarized cells (Fig. 5). Polarized CEACAM1-S-expressing cells were hardly stained at all (Fig. 5). Thus, the epitope recognized by Mab 5.4 was masked to a large extent under these conditions. In an attempt to investigate whether this might be due to homophilic binding between the N-terminal Ig-domains, we subjected confluent polarized cells to osmotic shrinkage by treatment with hyperosmotic sucrose, with the aim of physically breaking lateral cell-cell contacts. This resulted in a strong staining of CEACAM1-L with Mab 5.4 on the lateral surfaces (Fig. 5). Staining for occludin after sucrose treatment showed that the tight junctions were still intact (Fig. 6), and therefore the lateral staining of CEACAM1-L by Mab 5.4 was only detected after methanol permeabilization. Since, the tight junctions were intact there would be no re-localization of apical CEACAM1-L, but the hyperosmotic treatment of confluent cells caused an unmasking of the N-domain epitope on laterally localized CEACAM1-L.

The expression of CEACAM1-L in the lateral domain of polarized MDCK cells in a state in which the N-domain epitope was blocked and its unmasking by hyperosmotic sucrose suggested that this reflected involvement of CEACAM1-L in cell-cell adhesion. The question was raised whether this was caused by homophilic binding between the N-domains of CEACAM1-L molecules on opposing cell surfaces or whether CEACAM1-L bound to some other ligand presented by the adjacent cell.

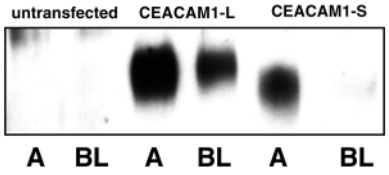


**Fig. 4.** Surface labelling of CEACAM1-L and CEACAM1-S expressing MDCK cells. Untransfected MDCK cells and MDCK cells transfected with CEACAM1-L or CEACAM1-S were grown to confluence on permeable filters and incubated with anti-CEACAM1 Fab fragments from either the apical (A) or the basolateral (BL) compartments. The cells were solubilized, bound Fab fragments were retrieved, and complexed CEACAM1 was detected by immunoblotting. No immunoreactive proteins were detected in the untransfected cells. In the transfected cells, CEACAM1-L was retrieved both from the apical and the basolateral surfaces, whereas CEACAM1-S was retrieved only from the apical surfaces.

To answer this question we made confluent, polarized cell layers from a 50:50 mixture of CEACAM1-L transfected and untransfected cells. This resulted in a monolayer composed of islands of CEACAM1-L-expressing and non-expressing cells that were in contact and joined by tight junctions evident from the occludin staining pattern (Fig. 7). CEACAM1-L-

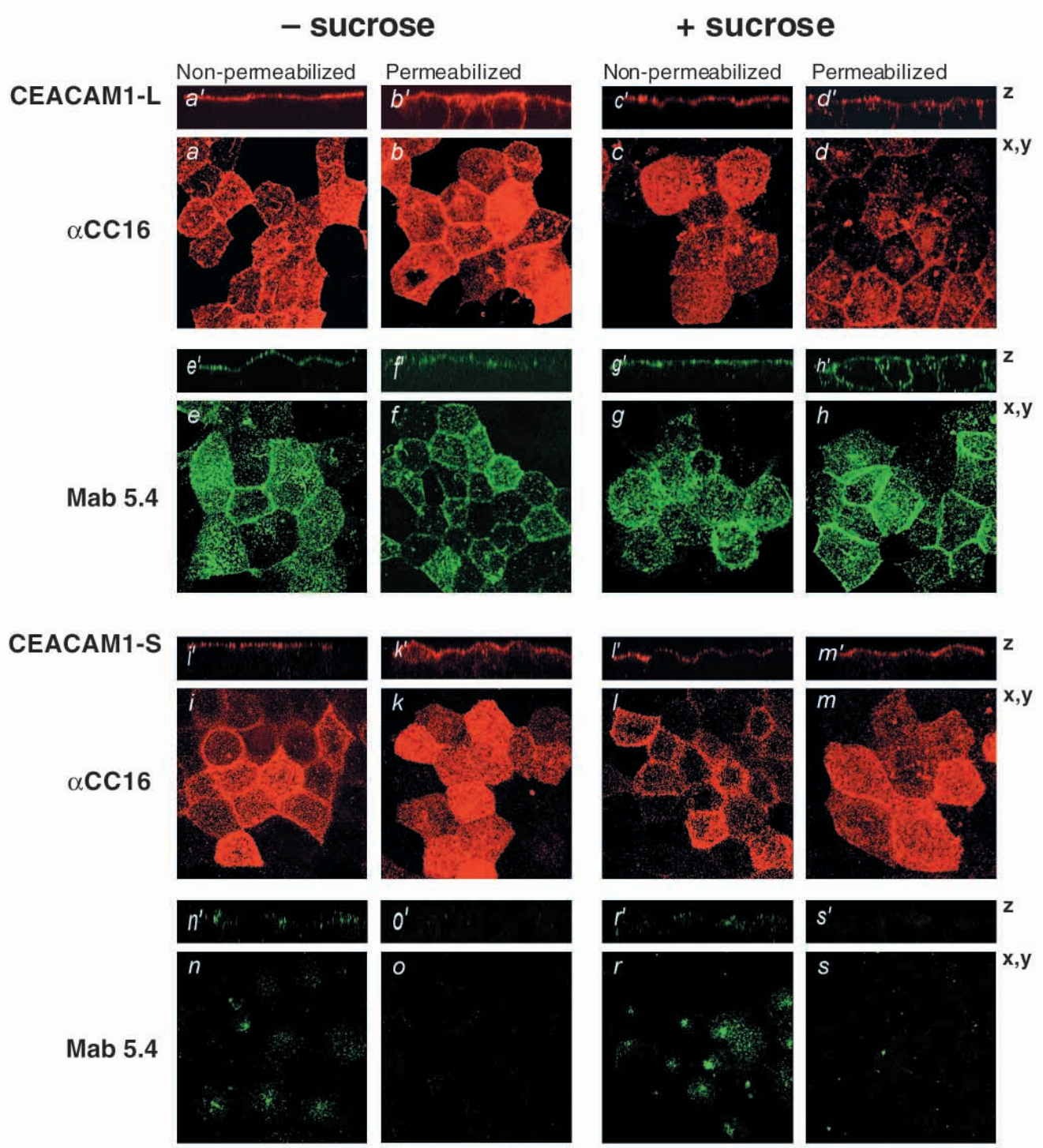


**Fig. 5.** Differential staining of CEACAM1 by polyclonal and monoclonal antibodies, and effects of hyperosmotic treatment. Confluent, polarized CEACAM1-L- or CEACAM1-S-expressing MDCK cells were treated with or without hyperosmotic sucrose, fixed with 3% paraformaldehyde and immunostained with or without methanol permeabilization. The cells were stained either with the polyclonal antibody αCC16 and Alexa546-conjugated secondary antibodies or with the monoclonal antibody 5.4 and Alexa488-conjugated secondary antibodies. For each sample both a z-reconstruction (a′-s′) and a composite xy-field (a-s) is shown. The composite xy-fields were constructed by simultaneously showing all xy focal planes of a visual field superimposed in a single, combined xy-field. Lateral staining for CEACAM1-L was seen with αCC16 both with and without sucrose treatment (b,b′,d,d′), although the staining was weaker after sucrose treatment. MAb 5.4 detected lateral staining of CEACAM1-L only after sucrose treatment (h,h′). Note that mAb 5.4 hardly stained CEACAM1-S at all, whether the cells were treated with hyperosmotic sucrose or not.

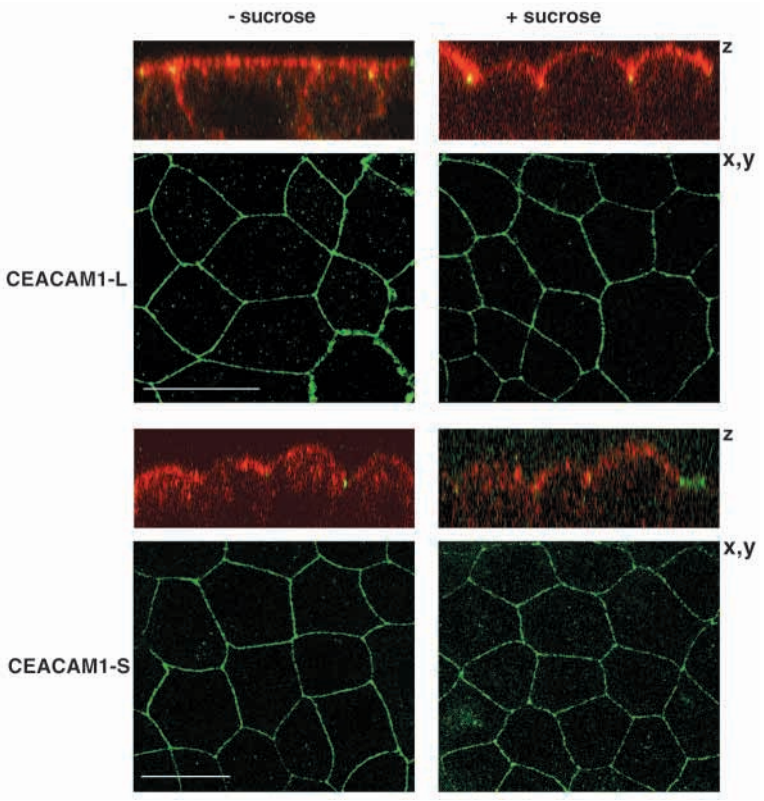


**Fig. 6.** Double-staining for CEACAM1 and occludin. Confluent, polarized CEACAM1-L- or CEACAM1-S-expressing MDCK cells were treated with or without hyperosmotic sucrose, fixed with 3% paraformaldehyde and permeabilized by methanol for 2 minutes at room temperature. They were then double-stained with an anti-occludin antibody and Alexa488-conjugated secondary antibodies (green colour) and anti-CEACAM1 (αCC16) and Alexa546-conjugated secondary antibodies (red colour). The z-reconstructions show the stainings for both CEACAM1 (red) and occludin (green). The xy-fields show focal planes at the level of the tight junctions; only the staining for occludin (green) is shown in these fields. The tight junctions were intact after treatment with hyperosmotic sucrose, as judged by the occludin staining. Note also that the lateral staining for CEACAM1-L is weaker after sucrose treatment. Bars: 20 μm.

expressing and non-expressing cells could clearly be distinguished because the strong apical staining for CEACAM1 was completely missing in the non-expressing cells. As before, lateral localization of CEACAM1-L was seen between two CEACAM1-L-expressing cells (Fig. 7). However, the borders between CEACAM1-L-expressing and non-expressing cells were completely free of CEACAM1-L, as judged by the lack of staining with either the polyclonal or the monoclonal antibodies, even after sucrose treatment (Fig. 7). Thus, it appears that CEACAM1-L did not bind to any other cell surface molecule on adjacent MDCK cells and that homophilic binding between opposing CEACAM1-L molecules was necessary for their maintenance at the lateral cell borders. This result also demonstrated that rat CEACAM1-L did not recognize and bind to endogenous canine CEACAM1.

Similar experiments with a mixture of CEACAM1-S-transfected and untransfected cells showed no lateral staining between expressing and non-expressing cells under any conditions (Fig. 7).

## CEACAM1-L appears in two different conformational or supramolecular states

Apically localized CEACAM1-L in polarized cells was stained by Mab 5.4, but significantly fewer cells were stained by 5.4 than by αCC16. In addition, the 5.4 staining was weaker and more patchy than the more homogeneous staining seen with αCC16 (Figs 5, 7). Taken together with the masking of the N-terminal epitope in the lateral location, this indicates that CEACAM1-L occurs in at least two different conformational or supramolecular organizational states in polarized MDCK cells. In order to analyze the topographical relationship between these two states, we performed double-staining with the two antibodies, Mab 5.4 and αCC16. The cells were first stained with the monoclonal antibody and then with the polyclonal antibody. In this double-staining procedure the monoclonal antibody showed the unmasked N-terminal epitope (denoted N-epitope), whereas the polyclonal antibody detected all other epitopes (denoted O-epitopes) except the N-terminal one. (If the order of staining was reversed, i.e. the cells were first stained with αCC16 and then with 5.4, no staining with the monoclonal antibody was observed, because the polyclonal αCC16 contained N-domain-recognizing antibodies that blocked binding of the monoclonal antibody.) When the two staining patterns were superimposed it became apparent that the majority of the apically localized CEACAM1-L exhibited O-epitopes (Fig. 8A), a minor portion of CEACAM1-L exhibited only the N-epitope, and in several locations there was an apparent colocalization between the N- and the O-epitopes when standard resolution (volume element (voxel): 0.07 μm/0.07 μm/0.35 μm, x/y/z; or 0.07 μm/0.07 μm/0.2 μm, x/y/z) was used (Fig. 8A,B). However, when the cells were viewed at the highest resolution (voxel: 0.04 μm/0.04 μm/0.2 μm, x/y/z), no colocalization of the two states were seen within the distinct volume elements (Fig. 8B). Thus, at the apical surface there was no molecular state in which the N- and the O-epitopes were exposed at the same time, and therefore CEACAM1-L seemed to appear in two mutually different conformational or supramolecular states in which either the N-epitope or the O-epitopes were exposed.

Using the double-staining procedure with the monoclonal/polyclonal anti-CEACAM1 antibodies, we found that hyperosmotic sucrose treatment led to masking of the O-epitopes and exposure of the N-epitopes of CEACAM1-L to a high extent in the lateral domain below the tight junction, but to a much lower extent in the apical domain above the tight junction (Fig. 8C). Thus, hyperosmotic sucrose treatment caused an almost complete shift of the supramolecular/conformational state of laterally localized CEACAM1-L from the O-epitope state to the N-epitope state.

## Confluent MDCK cell layers are a mosaic of cells with different supramolecular/conformational states of apically localized CEACAM1

The observation that Mab 5.4 did not stain confluent,

polarized CEACAM1-S-expressing cells under any conditions indicated that the N-epitope of apically localized CEACAM1-S was blocked in a similar way to those in laterally localized CEACAM1-L, whereas the O-epitopes were exposed. Apically localized CEACAM1-L, however, appeared in two states with either the N-epitope or the O-epitopes exposed, as described above. Interestingly, the cells were heterogeneous with respect to the balance of these two supramolecular/conformational CEACAM1-L states (Fig. 8A). The majority of the cells in an unperturbed monolayer exhibited essentially only the open O-epitope state, a significant proportion exhibited both supramolecular/conformational states, whereas the open N-epitope state dominated in a minority of the cells. This mosaic pattern was seen in all filter cultures that were analyzed. Since these transfected cell clones were monoclonal, this observation suggests that the cells in a monolayer appear in different states with respect to which CEACAM1-L organizational state dominates.

## Discussion

The two CEACAM1 cytoplasmic domain isoforms, CEACAM1-L and CEACAM1-S, exhibited different surface expression patterns when expressed in completely polarized MDCK cells. Both isoforms were expressed on the apical surfaces in high concentrations. In addition, CEACAM1-L became localized to the lateral cell surfaces, as unambiguously demonstrated both by confocal microscopy and by surface labelling experiments of intact, viable cells. How do these results agree with previously published data on the surface localization of CEACAM1 in polarized epithelial cells? In simple epithelial cells, such as small intestinal epithelial cells and renal proximal tubular epithelial cells, a strong staining is observed on the apical, brush-border carrying surface (Odin et al., 1988). A topologically identical localization is observed in the bile canalicular membranes of mature hepatocytes (Odin et al., 1988). However, very weak stainings have also been observed in the lateral surfaces of intestinal epithelial cells (Hansson et al., 1989), in mammary gland epithelial cells

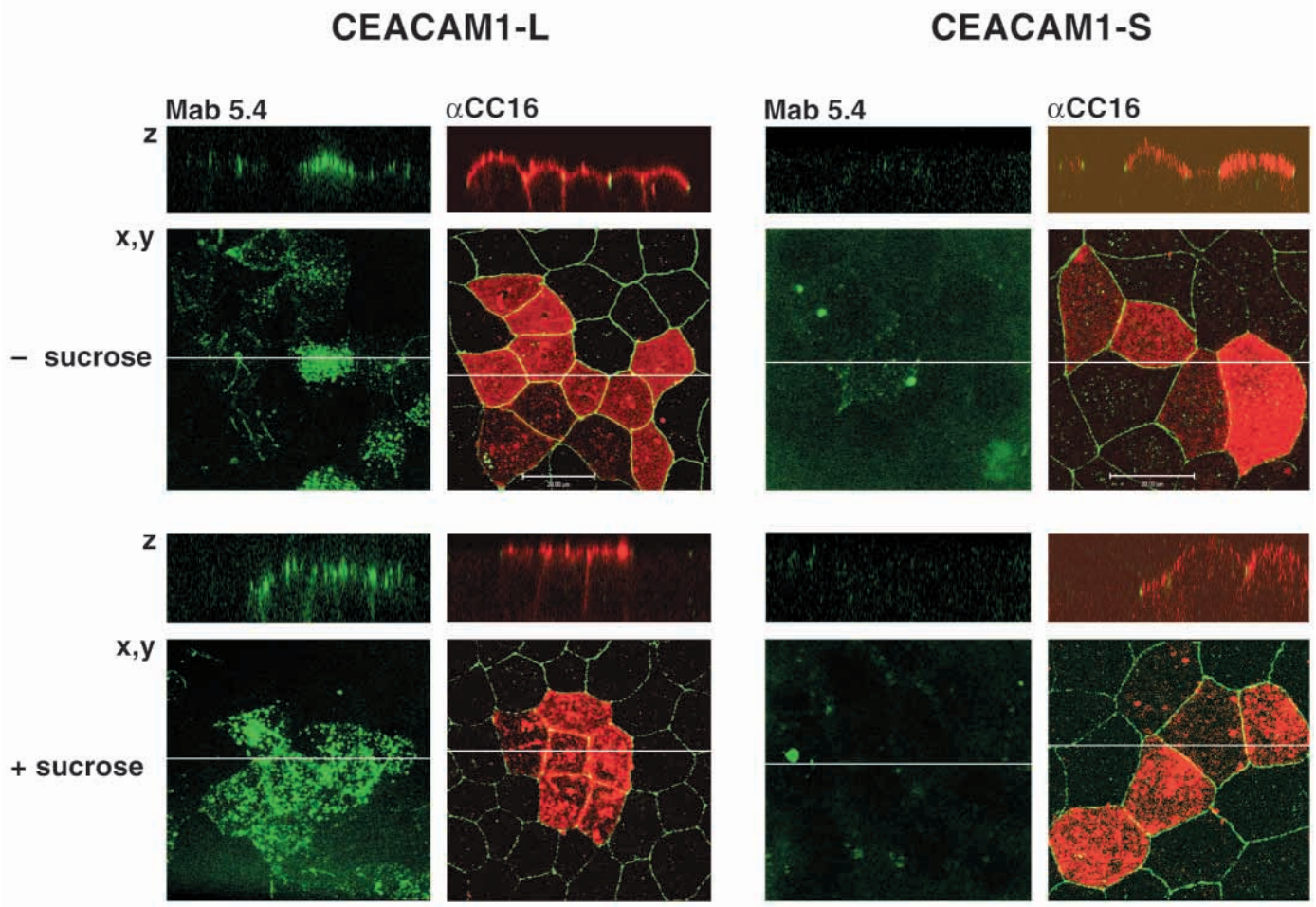


**Fig. 7**. Confocal microscopy of mixed CEACAM1-transfected and untransfected MDCK cells. Untransfected MDCK cells were mixed 50:50 with either CEACAM1-L-transfected or CEACAM1-S-transfected MDCK cells and grown to confluence on permeable filters. The cells were treated with or without hyperosmotic sucrose, fixed with 3% paraformaldehyde and permeabilized by methanol for 2 minutes at room temperature. Some cultures were stained with anti-CEACAM1 mAb 5.4/Alexa488-conjugated secondary antibodies (green colour), and some cultures were double-stained with anti-CEACAM1 αCC16/Alexa 546-conjugated secondary antibodies (red colour) and anti-occludin/Alexa488-conjugated secondary antibodies (green colour). The horizontal lines in the xy-composites indicate the plane for the z-reconstructions. Note that lateral expression of CEACAM1-L is only found in the borders between CEACAM1-L expressing cells but not in the borders between CEACAM1-L expressing cells and untransfected cells. CEACAM1-S was not stained by mAb 5.4. Bars: 20 μm.

(Huang et al., 1999) and in hepatocytes (Ocklind et al., 1983), by conventional immunohistochemical staining. Furthermore, Mowery and Hixson (Mowery and Hixon, 1991) demonstrated that CEACAM1 is expressed at a fairly high concentration in the lateral membrane of hepatocytes but in a state in which the epitope for an N-domain-recognizing monoclonal antibody is masked, unless adjacent cells are mechanically dissociated. However, they could not discriminate between the different CEACAM1 isoforms in their study. Several reports have demonstrated that epithelial cells express more S-isoform than L-isoform (Baum et al., 1996; Singer et al., 2000). Thus, if the L-isoform is distributed between the apical and lateral surfaces and the S-isoform is exclusively present in the apical surface, as demonstrated in the present investigation, there would be quantitatively much more total CEACAM1 present in the apical surface than in the lateral surface. Using antibodies that do not discriminate between the different isoforms, one would accordingly see a more intense staining in the apical surfaces than in the lateral surfaces. In addition, it is important to pay attention to our finding that insufficient fixation may lead to loss of membrane-bound proteins if detergent-permeabilization procedures are used. This would make a weak signal even weaker, which would also contribute to a scenario with an apparent lack of CEACAM1 expression in lateral membranes. Taken together, these observations are thus in excellent agreement with the present results, and we conclude that all available data are compatible with localization of CEACAM1-L both in the lateral and apical surfaces, whereas CEACAM1-S becomes expressed exclusively in the apical surface of polarized epithelial cells.

The signal for lateral localization must reside in the cytoplasmic domain of CEACAM1-L, as CEACAM1-L and CEACAM1-S are identical both in their extracellular and transmembrane domains. However, the intracellular signal(s) seems to be necessary but not sufficient for lateral localization, because there was no localization of CEACAM1-L to lateral borders between CEACAM1-L-expressing and non-expressing cells. This strongly suggests that homophilic, antiparallel binding is a prerequisite for maintaining CEACAM1-L at this location and furthermore emphasizes that laterally localized CEACAM1-L indeed was engaged in homophilic, antiparallel binding between adjacent cells. A similar observation was made by Sadekova et al. (Sadekova et al., 2000) in a completely different cell system. They expressed CEACAM1-L by microinjection into fibroblastic 3T3 cells and found that self-association of CEACAM1-L was necessary for its maintenance at sites of cell-cell contact.

One factor that might regulate the cell surface localization of the CEACAM1 isoforms is the interactions with the submembraneous cytoskeleton. Several investigators have found that CEACAM1 can bind to actin filaments (Hunter et al., 1994; DaSilva-Azevedo and Reutter, 1999; Schumann et al., 2001) and Sadekova et al. found that Rho family GTPases induce a relocalization of CEACAM1-L from intracellular sites to the cell surface in 3T3 cells (Sadekova et al., 2000). Our finding that CEACAM1-L was more firmly associated with the membrane cortex than CEACAM1-S are compatible with a role for the actin filament system in the differential surface localization of the two isoforms. Work is now in progress to identify the sites and amino-acid sequences in the cytoplasmic domain of CEACAM1-L that are important for its localization to the lateral domains, as well as for its interactions with the cell cortex.

Our finding that CEACAM1-L occurred in two different states is of great interest. The state in which the N-domain epitope (the N-epitope) was blocked was clearly involved in homophilic, antiparallel binding between adjacent cells, which is reasonable since it has been demonstrated that homophilic binding is mediated by a reciprocal binding between the N-domains of CEACAM1 molecules presented by opposing membranes (Wikström et al., 1996). In this state the other epitopes (the O-epitopes), recognized by the polyclonal antibodies, were accessible. In the state where the N-epitope was exposed it was intriguing to find that the O-epitopes were blocked. Interestingly, we did not observe any states in which both the N-epitope and the O-epitopes were exposed simultaneously. Although these two states might be explained by switching between different conformations, the simplest explanation is that they reflect monomeric and dimeric/oligomeric forms of CEACAM1-L. We have previously demonstrated that CEACAM1 can form parallel dimers in the plane of the membrane (Hunter et al., 1996). Although monomers and dimers are in mass-action-regulated equilibrium with each other, we showed that the cells could influence the extent of dimerization (Hunter et al., 1996). Furthermore, we found that the monomeric forms of CEACAM1 can mediate cell-cell adhesion by antiparallel, homophilic binding between N-domains (Hunter et al., 1996; Wikström et al., 1996). Thus, the state in which the N-epitope was blocked and the O-epitopes were exposed might represent antiparallel, homophilic binding between monomers, whereas the state in which the N-epitope was exposed and the O-epitopes were blocked could represent parallel dimers or clustered oligomers that did not participate in antiparallel, homophilic binding. The masking of the O-epitopes could then be explained by blocking owing to dimerization or oligomerization. According to the present results, monomeric CEACAM1 would then only exist when antiparallel, homophilic binding occurs between adjacent membranes. In the absence of antiparallel binding, CEACAM1 would be driven into the dimer state or clusters of parallel oligomers.

A reasonable explanation for the effect of hyperosmotic treatment on the organizational state of CEACAM1 is that shrinkage of the cells caused a mechanical rupture of the antiparallel, homophilic bonds between the CEACAM1-L molecules in the lateral cell surface domains. This would cause CEACAM1 to switch from antiparallel-bound monomers to dimers/oligomers not engaged in cell-cell binding. Such an explanation is supported by the observation that the hyperosmotic treatment caused a much more pronounced change of the CEACAM1-L organizational state in the lateral cell-cell contact areas than above the tight junctions (Fig. 8C). However, the hyperosmotic treatment might also affect the organization of CEACAM1-L in other ways. Cells have osmotic sensors, and several signaling pathways, including the classical MAP kinase pathway, are triggered by increased extracellular osmotic pressure (Roig et al., 2000; van der Wijk et al., 2000; Weiergräber and Häussinger, 2000). This might lead to altered phosphorylation of the cytoplasmic domain of CEACAM1-L, which in turn could change the monomer/dimer equilibrium and facilitate dimer/oligomer formation and breaking of homophilic, antiparallel bonds.

The two different organizational states of CEACAM1-L were also observed in the apical surfaces of the polarized MDCK cells, which suggest that the homophilic, antiparallel binding state exists, and even dominates, in this location as well. While, at the first glance this seems illogical, it can easily be explained as an interaction between adjacent membranes of the apical microvilli. When MDCK cells polarize, densely clustered microvilli of uniform size are developed in a brush-border-like configuration on the apical surfaces (Butor and Davoust, 1992). Our present confocal microscopical data showed that both isoforms of CEACAM1 were expressed along the entire length of the apical microvilli of the polarized MDCK cells. Immunoelectron microscopy has demonstrated that endogenous CEACAM1 is abundantly expressed along the sides of the microvilli as wells as in intestinal epithelial cells and hepatocytes (B.O., unpublished) (Kuprina et al., 1990; Mowery and Hixson, 1991; Frängsmyr et al., 1999), and we have previously suggested that CEACAM1 may mediate adhesive bonds between adjacent microvilli (Hansson et al., 1989). In intestinal and renal tubular brush borders, microvilli are closely arranged in a hexagonal pattern, and unidentified surface molecules on the microvillar membranes form bridges between adjacent microvilli (Copenhaver et al., 1971). In order to test whether this model would be compatible with the

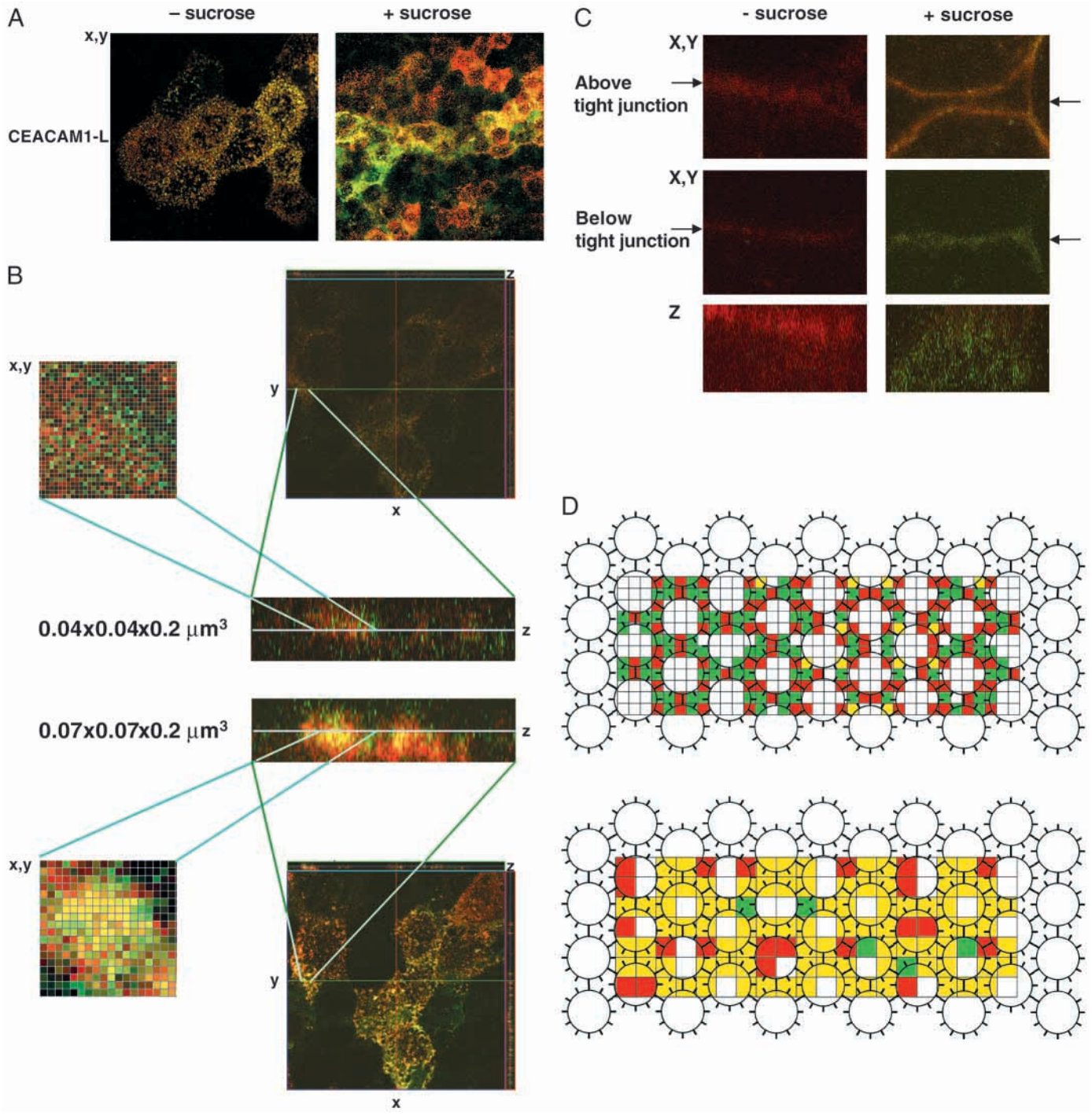

present data and could offer an explanation to the high resolution confocal staining patterns of CEACAM1 in the apical MDCK cell surfaces, we constructed the model that is shown in Fig. 8D. In this model we have drawn microvilli, the intermicrovillar distances and CEACAM1 to scale. The average diameter of brush border microvilli is 150 nm, the smallest intermicrovillar distance is around 30 nm, and the length of the 4 Ig domain extracellular domain of CEACAM1 is approximately 15 nm (from homology with the structure of CEA as solved by Bates et al. (Bates et al., 1992) and Boehm et al. (Boehm et al., 1996). The hexagonal arrangement of the microvilli allow for antiparallel CEACAM1-CEACAM1 binding at the narrowest inter-microvillar distances, whereas at other locations CEACAM1 would not be engaged in antiparallel binding. We then put a raster on this model with squares corresponding to 40×40 nm or 70×70 nm. Squares (pixels) that contained only antiparallel, bound CEACAM1 (corresponding to the state with masked N-epitope and exposed O-epitopes) were given a red color, squares (pixels) that contained only CEACAM1 not engaged in antiparallel binding (corresponding to the state with exposed N-epitope and masked O-epitopes) were given a green color, and squares (pixels) that contained both states of CEACAM1 were given a yellow color (no color grades owing to varying relative amounts of the two states within distinct pixels were introduced in this model). This showed that with a pixel size of 70×70 nm the majority of the pixels became yellow, whereas pixels of 40×40 nm became almost exclusively red or green. Given that the plastic microvilli are not perfectly circular in cross-section and not organized in an absolute hexagonal pattern, this is exactly the pattern that is seen in Fig. 8B. Accordingly, this analysis lends support to a model in which CEACAM1 mediates adhesive binding between closely packed microvilli on the apical surfaces of polarized epithelial cells.

Interestingly, CEACAM1-S seemed to be almost exclusively in the adhesive state in the apical surfaces, whereas CEACAM1-L occurred both in the adhesive and non-adhesive states, although the adhesive state dominated (Fig. 8A). This indicates that CEACAM1-S has a stronger tendency to form adhesive bonds, when in a cellular context, than CEACAM1-L, a tendency that also has been observed in direct cell adhesion experiments (Wikström et al., 1996). The monomer/dimer model can rationally explain this difference between the two isoforms. Both the extracellular domain of CEACAM1, which is identical in the two isoforms, and the cytoplasmic L-domain, which is lacking in CEACAM1-S, contribute to dimer formation (Hunter et al., 1996) (I. Hunter and B.O., unpublished). Therefore, CEACAM1-L has a stronger tendency to form dimers than CEACAM1-S. The monomer/dimer equilibrium would then be more shifted towards monomer formation for CEACAM1-S than for CEACAM1-L, which in turn would favor homophilic adhesion. Obviously, in this model coexpression of the two isoforms that allow for heterodimer formation would alter the balance between the adhesive and non-adhesive states

The observation that confluent monolayers of monoclonal, polarized CEACAM1-L-expressing cells constituted a mosaic of cells in which either the adhesive or the non-adhesive state of CEACAM1-L dominated suggests that the cells can regulate the adhesive properties of CEACAM1 in a dynamic manner. Cycling of CEACAM1 between adhesive and non-adhesive states might regulate microvillar motility, which could have an important function for stirring of the liquid layer close to the apical cell surface. This would facilitate absorption processes. The osmotic regulation of the adhesive state of CEACAM1 suggests that osmotic pressure could be a controlling factor for nutrient absorption by the small intestinal epithelial cells, which are constantly subjected to variations in the extracellular osmotic pressure owing to exposure to digested food stuffs.

**Fig. 8.** Double-staining for CEACAM1-L with monoclonal and polyclonal anti-CEACAM1 antibodies.Confluent, polarized CEACAM1-L-expressing cells were first stained with mAb 5.4/Alexa488-conjugated secondary antibodies (green colour), then with αCC16/Alexa546-conjugated secondary antibodies (red colour). The yellow colour indicates apparent colocalization. (A) Non-permeabilized cells, which were treated with or without hyperosmotic sucrose, were analyzed at standard resolution (voxel: 0.07×0.07×0.35 $\mu m^3$). A composite of all the focal planes for the entire apical region above the tight junction is shown for each sample. (B) Non-permeabilized cells, treated with hyperosmotic sucrose. Several focal planes (0.2 μm) were scanned through the apically located microvillar region, at two different xy-resolutions. In the upper part of the figure the higher resolution corresponds to a voxel size of 0.04×0.04×0.2 $\mu m^3$; in the lower part of the figure the same cells were scanned at lower resolution corresponding to a voxel size of 0.07×0.07×0.2 $\mu m^3$. The z-reconstructions through the microvillar region are from the same z-plane, as indicated by the horisontal lines in the xy-panels. Note that the apparent colocalization of the different epitopes at the lower resolution disappeared at the higher resolution. (C) Permeabilized cells treated with or without hyperosmotic sucrose. Voxel size, 0.04×0.04×0.2 $\mu m^3$. The upper panels (marked 'Above tight junction') represent an xy-plane through the apical portion of two adjacent cells. The middle panels (marked 'Below tight junction') represent an xy-plane through the middle portion of the same cells, half-way between the apical and the basal surfaces. The lower panels (marked z) represent a z-reconstruction through the border between the adjacent cells at the location indicated by the arrows in the upper and middle panels. Note that in the non-treated cells only the polyclonal epitopes (O-epitopes) were exposed, whereas in cells treated with hyperosmotic sucrose the monoclonal epitope (N-epitope) became exposed in the area below the tight junctions. (D) A model of apical microvilli analyzed at two pixel sizes. The microvilli of the apical surfaces in kidney tubular cells are uniform in size and organized in a hexagonal pattern. Here we show an xy-plane through the apical region, where we have drawn the microvilli, the intermicrovillar distances and CEACAM1 to scale. The average diameter of brush border microvilli is 150 nm, the smallest intermicrovillar distance is around 30 nm and the length of the 4 Ig domain extracellular domain of CEACAM1 is approximately 15 nm. The hexagonal arrangement of the microvilli allow for antiparallel CEACAM1-CEACAM1 binding at the narrowest inter-microvillar distances, while at other locations CEACAM1 would not be engaged in antiparallel binding. In the upper part of the figure we put a raster on this model with squares corresponding to 0.04×0.04 $\mu m^2$, in the lower part of the figure we put a raster on the model with squares corresponding to 0.07×0.07 $\mu m^2$, that is, the dimensions of the pixels in Fig. 8B. Squares (pixels) that contained only antiparallel, bound CEACAM1 (corresponding to the state with masked N-epitope and exposed O-epitopes) were given a red color, squares (pixels) that contained only CEACAM1 not engaged in antiparallel binding (corresponding to the state with exposed N-epitope and masked O-epitopes) were given a green color and squares (pixels) that contained both states of CEACAM1 were given a yellow color. This showed that with a pixel size of 0.07×0.07 $\mu m^2$ , the majority of the pixels became yellow, whereas the pixels of 0.04×0.04 $\mu m^2$ became almost exclusively red or green. See the Discussion for further details.

This work was supported by grants from the Swedish Medical Research Council (project no 05200), the Swedish Natural Science Research Council (project no B 5107), the Swedish Cancer Foundation (project no 3957) and Polysackaridforskning AB. We are grateful to Inga and Arne Lundbergs Foundation that made possible the purchase of the Zeiss LSM 510 confocal microscope. We thank B. B. Singer for suggesting the Fab-binding experiments to distinguish between apical and lateral localization.

## References

**Bates, P. A., Luo, J. and Sternberg, M. J. E.** (1992). A predicted three-dimensional structure for the carcinoembryonic antigen (CEA). *FEBS Lett*. **301**, 207-214.

**Baum, O., Troll, S. and Hixson, D. C.** (1996). The long and the short isoform of cell-CAM 105 show variant-specific modifications in adult rat organs. *Biochem. Biophys. Res. Commun*. **227**, 775-781.

**Boehm, M. K., Mayans, M. O., Thornton, J. D., Begent, R. H. J., Keep, P. A. and Perkins, S. J.** (1996). Extended glycoprotein structure of the seven domains in human carcinoembryonic antigen by X-ray and neutron solution scattering and an automated curve fitting procedure: Implications for cellular adhesion. *J. Mol. Biol*. **259**, 718-736.

**Brümmer, J., Neumaier, M., Göpfert, C. and Wagener, C.** (1995). Association of pp60c-src with biliary glycoprotein (CD66a), an adhesion molecule of the carcinoembryonic antigen family downregulated in colorectal carcinomas. *Oncogene* **11**, 1649-1655.

**Butor, C. and Davoust, J.** (1992). Apical to basolateral surface area ratio and polarity of MDCK cells grown on different supports. *Exp. Cell Res*. **203**, 115-127.

**Caplan, M. J., Anderson, H. C., Palade, G. E. and Jamieson, J. D.** (1986). Intracellular sorting and polarized cell surface delivery of $Na^+K^+$-ATPase, an endogenous component of MDCK cell basolateral plasma membranes. *Cell* **46**, 623-631.

**Copenhaver, W. M., Bunge, R. P. and Bunge, M. B.** (1971). Bailey's textbook of histology. 16th edition. Fig. 16-40, page 446. The Willams & Wilkins Company, Baltimore, Maryland, USA.

**DaSilva-Azevedo, L. and Reutter, W.** (1999). The long isoform of the cell adhesion molecule C-CAM binds to actin. *Biochem. Biophys. Res. Commun*. **256**, 404-408.

**Edlund, M., Gaardsvoll, H., Bock, E. and Öbrink, B.** (1993). Different isoforms and stock-specific variants of the cell adhesion molecule C-CAM (cell-CAM 105) in rat liver. *Eur. J. Biochem*. **213**, 1109-1116.

**Edlund, M., Blikstad, I. and Öbrink, B.** (1996). Calmodulin binds to specific sequences in the cytoplasmic domain of C-CAM and down-regulates C-CAM self association. *J. Biol. Chem*. **271**, 1393-1399.

**Edlund, M., Wikström, K., Toomik, R., Ek, P. and Öbrink, B.** (1998). Characterization of protein kinase C-mediated phosphorylation of the short cytoplasmic domain isoform of C-CAM. *FEBS Lett*. **425**, 137-142.

**Ergün, S., Kilik, N., Ziegler, G., Hansen, A., Nollau, P., Götze, J., Wurmbach, J. H., Horst, A., Weil, J., Fernando, M. and Wagener, C.** (2000). CEA-related cell adhesion molecule 1: a potent angiogenic factor and a major effector of vascular endothelial growth factor. *Mol. Cell* **5**, 311-320.

**Frängsmyr, L., Baranov, V. and Hammarström, S.** (1999). Four carcinoembryonic antigen subfamily members CEA, NCA, BGP and CGM2, selectively expressed in the normal human colonic epithelium, are integral components of the fuzzy coat. *Tumor Biol*. **20**, 277-292.

**Hansson, M., Blikstad, I. and Öbrink, B.** (1989). Cell-surface location and molecular properties of cell-CAM 105 in intestinal epithelial cells. *Exp. Cell Res*. **181**, 63-74.

**Hsieh, J. T., Luo, W., Song, W., Wang, Y., Kleinerman, D. I., Van, N. T. and Lin, S. H.** (1995). Tumor suppressive role of an androgen-regulated epithelial cell adhesion molecule (C-CAM) in prostate carcinoma cell revealed by sense and antisense approaches. *Cancer Res*. **55**, 190-197.

**Huang, J., Hardy, J. D., Sun, Y. and Shively, J. E.** (1999). Essential role of biliary glycoprotein (CD66a) in morphogenesis of the human mammary epithelial cell line MCF10F. *J. Cell Sci*. **112**, 4193-4205.

**Huber, M., Izzi, L., Grondin, P., Houde, C., Kunath, T., Veillette, A., Beauchemin, N.** (1999). The carboxyl-terminal region of biliary glycoprotein controls its tyrosine phosphorylation and association with protein-tyrosin phosphatases SHP-1 and SHP-2 in epithelial cells. *J. Biol. Chem*. **274**, 335-344.

**Hunter, I., Lindh, M. and Öbrink, B.** (1994). Differential regulation of C-CAM isoforms in epithelial cells. *J. Cell Sci*. **107**, 1205-1216.

**Hunter, I., Sawa, H., Edlund, M. and Öbrink, B.** (1996). Evidence for regulated dimerization of cell-cell adhesion molecule (C-CAM) in epithelial cells. *Biochem. J*. **320**, 847-853.

**Kunath, T., Ordonez-Garcia, C., Turbide, C. and Beauchemin, N.** (1995). Inhibition of colonic tumor cell growth by biliary glycoprotein. *Oncogene* **11**, 2375-2382.

**Kuprina, N. I., Baranov, V. N., Yazova, A. K., Rudinskaya, T. D., Escribano, M., Cordier, J., Gleiberman, A. S. and Goussev, A. I.** (1990). The antigen of bile canaliculi of the mouse hepatocyte: identification and ultrastructural localization. *Histochemistry* **94**, 179-186.

**Laemmli, U. K.** (1970). Cleavage of structural proteins during the assembly of the head of bacteriophage T4. *Nature* **227**, 680-685.

**Mowery, J. and Hixon, D. C.** (1991). Detection of cell-CAM 105 in the pericanalicular domain of the rat hepatocyte plasma membrane. *Hepatology* **13**, 47-56.

**Öbrink, B.** (1997). CEA adhesion molecules: Multifunctional proteins with signal-regulatory properties. *Curr. Opin. Cell Biol*. **9**, 616-626.

**Ocklind, C. and Öbrink, B.** (1982). Intercellular adhesion of rat hepatocytes. Identification of a cell surface glycoprotein involved in the initial adhesion process. *J. Biol. Chem*. **257**, 6788-6795.

**Ocklind, C., Forsum, U. and Öbrink, B.** (1983). Cell surface localization and tissue distribution of a hepatocyte cell-cell adhesion glycoprotein (cell-CAM 105). *J. Cell Biol*. **96**, 1168-1172.

**Odin, P., Tingström, A. and Öbrink, B.** (1986). Chemical characterization of cell-CAM 105, a cell adhesion molecule isolated from rat liver membranes. *Biochem. J*. **236**, 559-568.

**Odin, P., Asplund, M., Busch, C. and Öbrink, B.** (1988). Immunohistochemical localization of cell-CAM 105 in rat tissues. Appearence in epithelia, platelets and granulocytes. *J. Histochem. Cytochem*. **36**, 729-739.

**Olsson, H., Wikström, K., Kjellström, G. and Öbrink, B.** (1995). Cell adhesion activity of the short cytoplasmic domain isoform of C-CAM (C-CAM2) in CHO cells. *FEBS Lett*. **365**, 51-56.

**Phillips, M. J., Oshio, C., Miyairi, M., Katz, H. and Smith, C. R.** (1982). A study of bile canalicular contractions in isolated hepatocytes. *Hepatology* **2**, 763-768.

**Roig, J., Huang, Z., Lytle, C. and Traugh, J. A.** (2000). p21-activated protein kinase γ-PAK is translocated and activated in response to hyperosmolarity. *J. Biol. Chem*. **275**, 16933-16940.

**Sadekova, S., Lamarche-Vane, N., Li, X. and Beauchemin, N.** (2000). The CEACAM1-L glycoprotein associates with the actin cytoskeleton and localizes to cell-cell contact through activation of Rho-like GTPases. *Mol. Biol. Cell* **11**, 65-77.

**Sawa, H., Kamada, K., Sato, H., Sendo, S., Kondo, A., Saito, I., Edlund, M. and Öbrink, B.** (1994). C-CAM expression in the developing rat central nervous system. *Develop. Brain Res*. **78**, 35-43.

**Sawa, H., Ukita, H., Fukuda, M., Kamada, H., Saito, I. and Öbrink, B.** (1997). Spatiotemporal expression of C-CAM in the rat placenta. *J. Histochem. Cytochem*. **45**, 1021-1034.

**Schumann, D., Chen, C.-J., Kaplan, B. and Shively, J. E.** (2001). Carcinoembryonic antigen cell adhesion molecule 1 directly associates with cytoskeleton proteins actin and tropomyosin. *J. Biol. Chem*. **276**, 47421-47433.

**Singer, B. B., Scheffran, I. and Öbrink, B.** (2000). The tumor growth-inhibiting cell adhesion molecule CEACAM1 (C-CAM) is differently expressed in proliferating and quiescent epithelial cells and regulates cell proliferation. *Cancer Res*. **60**, 1236-1244.

**Skubitz, K. M., Campbell, K. D., Ahmed, K. and Skubitz, A. P. N.** (1995). CD66 family members are associated with tyrosine kinase activity in human neutrophiles. *J. Immunol*. **155**, 5382-5390.

**van der Wijk, T., Tomassen, S. F. B., deJonge, H. R. and Tilly, B. C.** (2000). Signalling mechanisms involved in volume regulation of intestinal epithelial cells. *Cell. Physiol. Biochem*. **10**, 289-296.

**Watanabe, N., Tsukada, N., Smith, C. R. and Phillips, M. J.** (1991). Motility of bile canaliculi in the living animal: Implications for bile flow. *J. Cell Biol*. **113**, 1069-1080.

**Weiergräber, O. and Häussinger, D.** (2000). Hepatocellular hydration: Signal transduction and functional implications. *Cell. Physiol. Biochem*. **10**, 409-416.

**Wikström, K., Kjellström, G. and Öbrink, B.** (1996). Homophilic intercellular adhesion mediated by C-CAM is due to a domain1-domain1 reciprocal binding. *Exp. Cell Res*. **227**, 360-366.